



ELSEVIER

SCIENCE @ DIRECT®

Journal of Theoretical Biology ■ (■■■■) ■■■-■■■

Journal of
Theoretical
Biologywww.elsevier.com/locate/jtbi

A reduced mathematical model of the acute inflammatory response: I. Derivation of model and analysis of anti-inflammation

Angela Reynolds^a, Jonathan Rubin^{a,*}, Gilles Clermont^{b,c,d}, Judy Day^a,
Yoram Vodovotz^{b,c,e}, G. Bard Ermentrout^a

^aDepartment of Mathematics, 301 Thackeray, University of Pittsburgh, Pittsburgh, PA 15260, USA

^bCIRM (Center for Inflammation and Regenerative Modeling), 100 Technology Drive Suite 200, Pittsburgh, PA 15219-3110, USA

^cCRISMA Laboratory, University of Pittsburgh, Pittsburgh, PA 15261, USA

^dDepartment of Critical Care Medicine, 3550 Terrace St., University of Pittsburgh Medical Center, Pittsburgh, PA 15261, USA

^eDepartment of Surgery, University of Pittsburgh Medical Center, W1542 Biomedical Sciences Tower, 200 Lothrop St., Pittsburgh, PA 15213, USA

Received 24 October 2005; received in revised form 18 February 2006; accepted 22 February 2006

Abstract

The acute inflammatory response, triggered by a variety of biological or physical stresses on an organism, is a delicate system of checks and balances that, although aimed at promoting healing and restoring homeostasis, can result in undesired and occasionally lethal physiological responses. In this work, we derive a reduced conceptual model for the acute inflammatory response to infection, built up from consideration of direct interactions of fundamental effectors. We harness this model to explore the importance of dynamic anti-inflammation in promoting resolution of infection and homeostasis. Further, we offer a clinical correlation between model predictions and potential therapeutic interventions based on modulation of immunity by anti-inflammatory agents.

© 2006 Elsevier Ltd. All rights reserved.

Keywords: Immunology; Mathematical modeling; Anti-inflammatory cytokines; Sepsis; Bifurcation analysis

1. Introduction

Acute biological stress, such as severe infection or trauma, leads to the development of an acute inflammatory response. The goal of this response is to promote adaptation of the organism to stress, eliminate threats to survival such as pathogens, and promote tissue repair and healing. However, an excessive or inappropriate inflammatory response will lead to collateral tissue damage, organ dysfunction, a prolonged healing phase, or possibly death. This state of excessive inflammation is particularly common in association with extensive physiological organ support as provided in modern intensive care units (Goris et al., 1985; Takala et al., 1999). Organisms have developed regulatory mechanisms to contain the molecular and cellular cascades initiated by excessive inflammation. In general, pro-inflammatory elements that are key to ridding

organisms of large numbers of pathogens also mobilize a negative feedback, or anti-inflammatory response, which downregulates the initial inflammatory wave (Fig. 1). Specific details of pro- and anti-inflammatory responses may be sculpted by the nature and magnitude of the initiating insults, as well as by genetic predispositions.

In prior work, we constructed a reduced mathematical model of the pro-inflammatory response (Kumar et al., 2004) consisting of a response instigator (pathogen) and early and late pro-inflammatory mediators. While that model captured a variety of clinically relevant scenarios associated with the inflammatory response to infection, the goal of the present work is to gain insight into the presumed advantage and robustness instilled by the presence of a time-dependent anti-inflammatory response. While anti-inflammation inhibits the subsequent build-up of pro-inflammation and the damage to tissue that may be caused by pro-inflammation, it also mitigates the subsequent production of anti-inflammatory mediators. Thus, the overall effects of anti-inflammation on the outcome following pathogenic infection, and how these

*Corresponding author. Tel.: +1 412 624 6157; fax: +1 412 624 8397.

E-mail address: rubin@math.pitt.edu (J. Rubin).

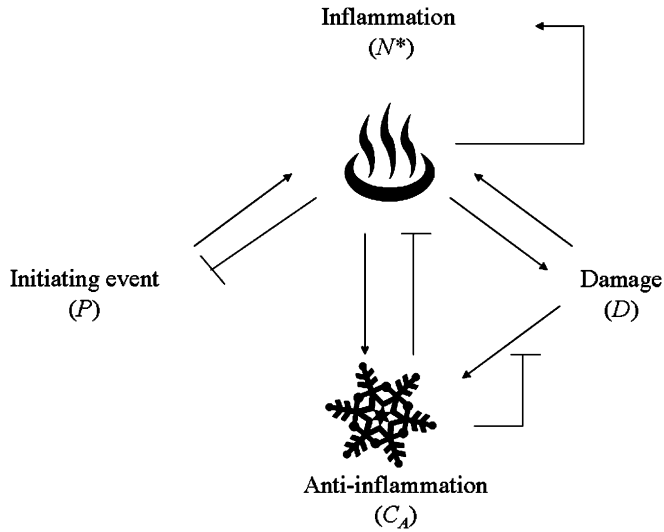


Fig. 1. Interactions included in our four-variable model of the acute immune response. Arrows and bars represent upregulation and inhibition, respectively. The bar between anti-inflammation and inflammation corresponds to the inhibition of both the production of inflammation and the ability of inflammation to interact with all other involved species.

effects depend on parameters such as pathogen growth rate and the anti-inflammatory response rate itself, may be difficult to predict by intuition alone but are well suited for dynamical systems analysis.

As the first step in performing this mathematical analysis, we derive a reduced model of the acute immune response that incorporates pro- and anti-inflammation. This model does not include components of the adaptive immune response, such as T-cells and specific antibodies. Therefore, this model describes the generic response to pathogenic insult (Janeway and Medzhitov, 2002). Our derivation proceeds through several stages, based on calibration of subsystems to generally accepted features of the interactions of particular immune system components, as observed in previous experimental studies. We construct a reduced model of inflammation from these subsystems, where the impact of dynamic anti-inflammation is evaluated through simulations and bifurcation studies. Our results illustrate the health advantage conferred by a dynamic anti-inflammatory response and suggest that the rates of this response may be well tuned to yield optimal outcomes following pathogenic infection. Our findings also point to risks associated with manipulation of the levels of the anti-inflammatory mediator present, either before an initial infection or following an initial infection that is on its way to, but has not yet reached, a healthy resolution. We conclude with a discussion in which we elaborate on these and other possible therapeutic implications of our results.

2. Methods

Our reduced model of the acute inflammatory response consists of a system of four differential equations in which

the dependent variables represent the levels of pathogen (P), activated phagocytes (N^*) such as activated neutrophils, tissue damage (D), and anti-inflammatory mediators (C_A) such as cortisol and interleukin-10. This model describes the interactions depicted in Fig. 1. We develop this model by first considering the two-variable subsystems N^*/P and N^*/D , treating C_A as a parameter, then combining these subsystems to form a three-variable subsystem, and finally incorporating the dynamics of the anti-inflammatory mediator to create the reduced model. We adopted a subsystem approach to ensure that the interactions of the model variables are consistent with biological observations.

Baseline parameter values for both the subsystems and the reduced model are provided in Table 1 and are selected to remain within the given ranges and constraints found in the experimental literature. This baseline parameter set is used for all simulations except where noted in the text. Parameters that could not be documented from existing data were estimated such that the subsystems behave in a biologically appropriate manner for plausible levels of the anti-inflammatory mediators. Furthermore, when the pathogenic insult is replaced by endotoxin as an initiating event, as presented in Day et al. (2006), the resulting model qualitatively reproduces the responses of immune mediators measured experimentally during repeated endotoxin administrations. Further details on the derivation of parameter ranges, constraints and estimated values, are presented in the Supplementary Materials. Units for the model variables and many of the associated parameters cannot be determined, since the variables represent various types of cells, signaling proteins such as cytokines, and/or other mediators concurrently. More precisely, these variables quantify the response of the immune function they represent rather than, for example, an exact cell count. Therefore, units of most parameters related to these variables are not in conventional form, but rather in terms of the associated variable.

Throughout the analysis of the reduced model and its subsystems, we will be tracking the existence and values of fixed points, determining the parameter regimes in which particular fixed points are stable, and locating bifurcations. A fixed point is a point where the derivatives of all variables in the system are zero, also known as a critical point or equilibrium point. This occurs where the nullclines¹ of the system intersect. We will refer to a fixed point as stable if the real part of each eigenvalue associated with the linearized system at that fixed point is negative. In the systems that we consider, it is exactly the stable fixed points that represent possible asymptotic steady states attained by open sets of initial conditions. A bifurcation

¹For a system of the form $dx/dt = f(x, y)$; $dy/dt = g(x, y)$, the x -nullcline (y -nullcline) is the set of points in the (x, y) plane that satisfy $f = 0$ ($g = 0$). Intersections of nullclines are fixed points, since at an intersection both dx/dt and dy/dt are zero. These ideas generalize directly to systems with more than two equations.

Table 1
Parameters

Parameter	Range	Value	Description	Comments	Sources
k_{pm}	Estimated	$0.6/M$ -units/h	Rate at which the non-specific local response (M) eliminates pathogen	Estimated to be considerably less efficient than a phagocyte-driven response, and therefore can be overwhelmed with modest to large inocula of pathogen	
k_{np}	Estimated	$0.01/P$ -units/h	Rate at which the non-specific local response is exhausted by pathogen (P)	Chosen to balance known natural half-life of non-specific antibodies (see below)	
s_m	Estimated	$0.005 M$ -units/h	Source of non-specific local response	Range based on the reported half-lives of immunoglobulins G and A, non-specific antibodies probably key in the non-specific local immune response	Janeway et al., 2001; Zouali, 2001
μ_m	0.0013–0.0048/h	0.002/h	Decay rate for the non-specific local response		
k_{pg}	0.021–2.44/h	Various	The growth rate of pathogen	Estimated from a lethal model of <i>E. coli</i> rat peritonitis	Spector, 1956; Todar, 2002
P_{∞}	Estimated	20×10^6 /cc	Maximum pathogen population		Vodovotz, Y. pers. comm.
k_{pn}	Maximum 2.5/ N^* -units/h	$1.8/N^*$ -units/h	Rate at which activated phagocytes (N^*) consume pathogen	Based on observed mean rate of phagocytosis by macrophages in the presence of unlimited supply of targets	Branwood et al., 1992
k_{np}	Estimated	$0.1/P$ -units/h	Activation of resting phagocytes (N_R) by pathogen		
k_{nn}	Estimated	$0.01/N^*$ -units/h	Activation of resting phagocytes by previously activated phagocytes and their cytokines		
s_{nr}	Estimated	$0.08 N_R$ -units/h	Source of resting phagocytes	This parameter was chosen to ensure a stable concentration of resting phagocytes in the absence of any perturbation on the system	
μ_{nr}	0.069–0.12/h	0.12/h	Decay rate of resting phagocytes	We used half-life of 6 h	Coxon et al., 1999
μ_n	Less than μ_{nr}	0.05/h	Decay rate of activated phagocytes	Activated cells have prolonged half-lives due to delayed apoptosis	Coxon et al., 1999
k_{nd}	Less than k_{np}	$0.02/D$ -units/h	Activation of resting phagocytes by tissue damage (D)	Peak of the activated phagocyte response elicited from pathogen (k_{np}) is greater than that triggered by damage (k_{nd})	Andersson et al., 2000

Table 1 (continued)

Parameter	Range	Value	Description	Comments	Sources
k_{dn}	Estimated	0.35 D -units/h	Maximum rate of damage produced by activated phagocytes (and/or associated cytokines and free radicals)		
λ_{dn}	Estimated	0.06 N^* -units	Determines level of activated phagocytes needed to bring damage production up to half its maximum		
μ_d	0.017 minimum	0.02/h	Decay rate of damage; a combination of repair, resolution, and regeneration of tissue	We calculated the parameter from data of the half-life of HMG-1, a histone tethering protein leaked by damaged cells as a surrogate for the many danger molecules that perpetuate the inflammatory signal	Wang et al., 1999
c_{∞}	Estimated	0.28 C_A -units	Controls the strength of the anti-inflammatory mediator (C_A)	Set such that $f(x) = x/(1 + (C_A/c_{\infty})^2)$ corresponds to $\approx 75\%$ inhibition when C_A reaches maximum value in response to an insult	Isler et al., 1999
s_c	Estimated	0.0125 C_A -units/h	Source of the anti-inflammatory mediator	Organisms have constitutive levels of anti-inflammatory effectors. The source parameter was chosen to balance their documented half-life	Tsukaguchi et al., 1999
k_{cn}	Estimated	0.04 C_A -units/h	Maximum production rate of the anti-inflammatory mediator		
k_{cnd}	Estimated	48 N^* -units/ D -units	Relative effectiveness of activated phagocytes and damaged tissue in inducing production of the anti-inflammatory mediator		
μ_c	0.15–2.19/h	0.1/h	Decay rate of the anti-inflammatory mediator	Anti-inflammatory signals have downstream cellular effects not explicitly modeled herein, lasting longer than the effector cytokine or molecule producing it. Therefore, our parameter value was set below the lower limit of reported half-lives of anti-inflammatory effectors. This still probably is a higher bound for this parameter	Bacon et al., 1973; Bocci, 1991; Fuchs et al., 1996; Huhn et al., 1997

occurs when a change in a parameter alters the number of fixed points and/or their stability, and thus changes the number and nature of the asymptotic steady states of the system (Strogatz, 1994).

The reduced model displays three physiologically relevant equilibrium points, which correspond to biological states of health, aseptic death, and septic death, respectively. The health state is a fixed point with $P = 0$, $N^* = 0$, $D = 0$, and $C_A = s_c/\mu_c$, which, when stable, is the desirable asymptotic behavior. The aseptic death state, which corresponds to an outcome where pathogen has been eliminated but with high and persistent immune activation and damage, is a fixed point where $P = 0$, $N^* > 0$, $D > 0$ and $C_A > 0$. The third possible equilibrium is septic death, where all variables are non-zero, which corresponds to a state in which there is insufficient immune activation to clear pathogen. Note that a healthy outcome viewed as a return to an equilibrium point is an idealized construct. In fact, the complex biological systems we are considering are out of equilibrium and a return to mediator levels within the basin of attraction² of the health state is a desirable outcome. However, in the reduced model, solutions with initial conditions in the basin of attraction of health asymptotically approach health. Thus, for simplicity we refer to the fixed point, $(0,0,0,s_c/\mu_c)$ as the health state.

2.1. The non-specific local immune response: the M/P subsystem

A normal individual in a healthy state has a baseline capacity to respond and resolve local infections. This resides in the presence of cells, such as tissue macrophages as well as other non-specific physical and biological defenses, such as defensins and non-specific antibodies (Ochsenbein and Zinkernagel, 2000; Paulsen et al., 2002; Raj and Dentino, 2002). This local response is rapid and effective, but can be overwhelmed with large inocula or rapidly dividing pathogens. To account for this non-specific local removal of pathogen, we assume the reactions in Table 2, with the non-specific local response and pathogen levels represented by the variables M and P , respectively.

From the reactions in Table 2, based on mass action kinetics, we derive the following preliminary equations:

$$\frac{dM}{dt} = s_m - \mu_m M - k_{mp}MP,$$

$$\frac{dP}{dt} = -k_{pm}MP.$$

For simplicity, we assume that the local response reaches quasi-steady state and substitute $M = s_m/(\mu_m + k_{mp}P)$ into the pathogen equation. Further, to incorporate the dynamics of the pathogen population into our model, we

Table 2

Reactions involving the local immune response (M) and pathogen (P)

$M + P \xrightarrow{k_{pm}} M$	P is destroyed at the rate k_{pm} when it encounters M
$M + P \xrightarrow{k_{mp}} P$	M is consumed at the rate k_{mp} when it encounters P
$* \xrightarrow{s_m} M$	Source of M
$M \xrightarrow{\mu_m}$	Death of M

used a logistic growth term, $k_{pg}P(1 - P/p_\infty)$. Therefore, we obtain the pathogen equation:

$$\frac{dP}{dt} = k_{pg}P \left(1 - \frac{P}{p_\infty}\right) - \frac{k_{pm}s_m P}{\mu_m + k_{mp}P}. \quad (1)$$

Here, the pathogen growth rate and the carrying capacity of the pathogen population are represented by k_{pg} and p_∞ , respectively. The units for k_{pg} are per hour while p_∞ has the same units as P , $10^6/\text{cc}$. $P = 0$ is always a fixed point of Eq. (1). We find that a saddle-node bifurcation gives rise to two additional fixed points, say $p_1 < p_2$, which exist for $k_{pg} > 4k_{mp}k_{pm}s_m p_\infty / (p_\infty k_{mp} + \mu_m)^2$, or equivalently for $k_{pg} > 0.059$ with the parameters in Table 1. When they first arise, p_1 and p_2 are positive. Direct linearization and algebraic manipulation show that $P = 0$ is stable for $k_{pg} < k_{pm}s_m/\mu_m = 1.5$, where it loses stability in a transcritical bifurcation with p_1 , and that the largest fixed point is stable whenever it exists. Thus for $0.059 < k_{pg} < 1.5$, this subsystem is bistable.

2.2. The N^*/P subsystem

A key component of the acute immune response is the removal of the pathogen by phagocytic immune cells, such as activated neutrophils and macrophages. Resting phagocytes are activated by pathogen and by previously activated phagocytes via the binding of endotoxin and pro-inflammatory cytokines (Janeway and Medzhitov, 2002). Once activated, a phagocyte becomes efficient at eliminating pathogens. When the growth rate of the pathogen is low, activated phagocytes are capable of clearing the pathogen in normal individuals. However, if the growth rate is high, then a sufficiently large inoculum of pathogen can induce a persistent infection despite the attack by activated phagocytes. This dependence on k_{pg} and the interaction between resting and activated phagocytes are essential in developing the N^*/P subsystem, which consists of the following:

$$\frac{dP}{dt} = k_{pg}P \left(1 - \frac{P}{p_\infty}\right) - \frac{k_{pm}s_m P}{\mu_m + k_{mp}P} - k_{pn}N^*P, \quad (2)$$

$$\frac{dN^*}{dt} = \frac{s_{nr}R_1}{\mu_{nr} + R_1} - \mu_n N^*, \quad (3)$$

where $R_1 = k_{nn}N^* + k_{np}P$.

To derive Eqs. (2) and (3) we first take into account the activation of the resting phagocytes (N_R). In particular, from the system of reactions given in Table 3, we derive the

²The basin of attraction of a stable fixed point, x^* , of a dynamical system is the set of all initial conditions that dynamically evolve to x^* (Strogatz, 1994).

Table 3
Reaction involving resting and activated phagocytes

$N_R \xrightarrow{k_{np}P+k_mN^*} N^*$	Activation of the resting phagocytes (N_R) is induced by the presence of pathogen (P) and by positive feedback from the activated phagocytes (N^*) via pro-inflammatory cytokines
$* \xrightarrow{s_{nr}} N_R$	Source of N_R
$N_R \xrightarrow{\mu_{nr}}$	Death of N_R
$N^* \xrightarrow{\mu_n}$	Death of N^*

following equations:

$$\frac{dN_R}{dt} = s_{nr} - \mu_{nr}N_R - R_1N_R,$$

$$\frac{dN^*}{dt} = R_1N_R - \mu_nN^*,$$

where $R_1 = k_mN^* + k_{np}P$.

When a resting phagocyte encounters an agent capable of activating it, however, the activation process is rapid. Thus, we assume that the variable N_R is in quasi-steady state, reducing the N_R/N^* system to a single equation (3). When this equation is combined with the pathogen equation (1) derived above, and an additional term is included to encode the direct consumption of pathogen by activated phagocytes, we obtain systems (2) and (3).

Linearization of Eqs. (2) and (3) about the health fixed point $(P, N^*) = (0, 0)$ yields real eigenvalues that are negative for $k_{pg} < k_{pm}s_m/\mu_m$ and $\mu_n > s_{nr}k_{nn}/\mu_{nr}$. Since the second of these inequalities holds for the parameters in Table 1, the condition $k_{pg} < k_{pm}s_m/\mu_m$ is once again the criterion for the stability of health, as in the M/P subsystem.

We provide a further analysis of the fixed points of Eqs. (2) and (3) below, but first, to more accurately model the immune response, we introduce the anti-inflammatory mediator in this subsystem. At this point, we simply encode anti-inflammatory effects in a parameter C_A . By treating the anti-inflammatory mediator as a parameter, we can manually manipulate it to verify that sustained variations in its level induce biologically appropriate alterations in the N^*/P dynamics, such that this subsystem will behave

appropriately once dynamic anti-inflammatory mediators are incorporated.

In normal individuals, the anti-inflammatory mediator inhibits the activation of phagocytes and reduce the ability of activated phagocytes to attack pathogen (Tsukaguchi et al., 1999). We incorporate this inhibition into the N^*/P subsystem by replacing R_1 with $f(R_1)$ and N^* with $f(N^*)$ in Eq. (2), for $f(V) = V/(1 + (C_A/c_\infty)^2)$. The parameter c_∞ is set such that when the anti-inflammatory mediators reach their maximum level in response to an infection, their inhibitory effects are roughly equivalent to a 75% reduction in the inhibited element, as seen in Isler et al. (1999). While it would have been reasonable to consider different levels of inhibition by the anti-inflammatory mediator for each interaction, we consider uniform inhibition for simplicity.

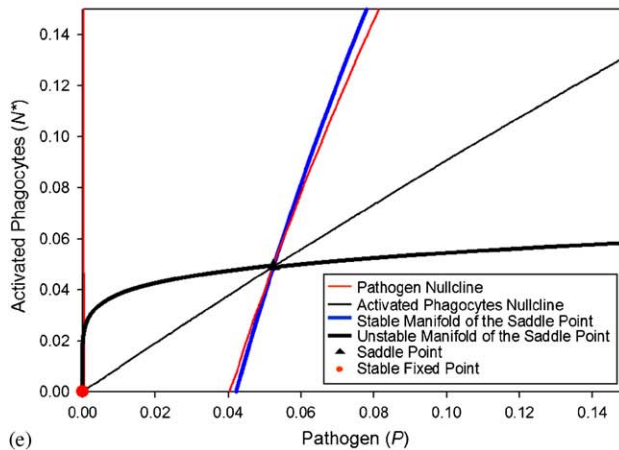
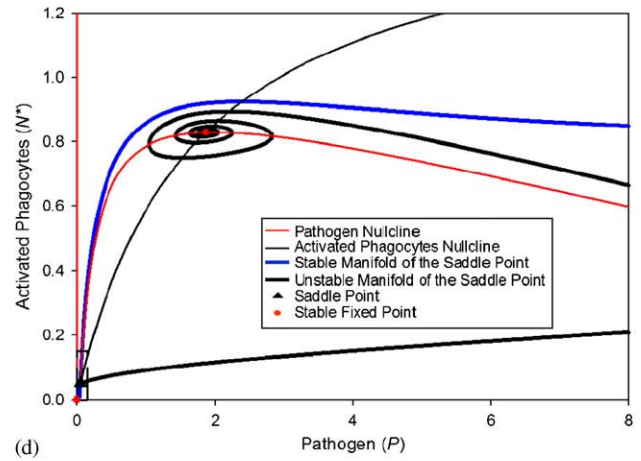
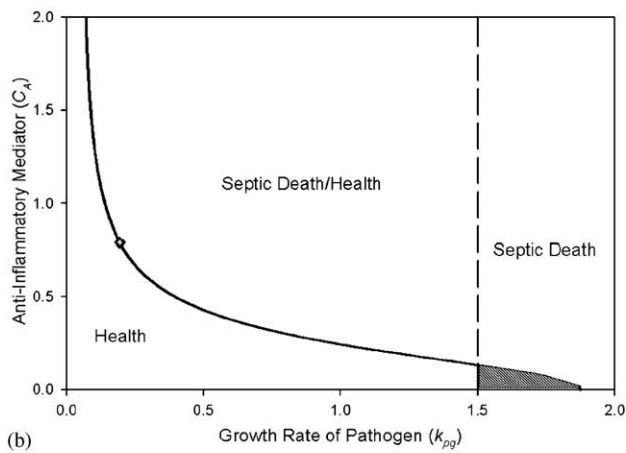
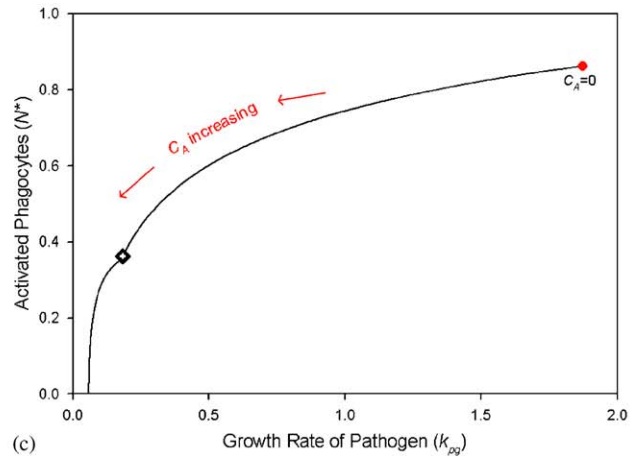
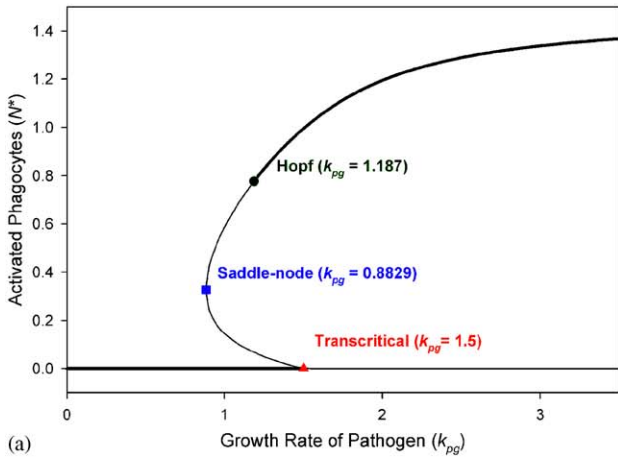
For low pathogen growth rate (k_{pg}), the resulting N^*/P subsystem has only the stable health state, whose existence is independent of C_A . There is a saddle-node bifurcation at $k_{pg} = 0.8829$ for the parameters in Table 1 with C_A fixed to 0.2. The corresponding bifurcation diagram is displayed in Fig. 2(a), which was created, as were all other figures in this paper, using XPPAUT (Ermentrout, 2002). Of the pair of fixed points born in the saddle-node bifurcation, the lower (with respect to N^*) is a saddle separatrix, while the upper, corresponding to septic death ($P > 0, N^* > 0$), is initially unstable. As k_{pg} increases further, there is a Hopf bifurcation at $k_{pg} = 1.187$, which stabilizes septic death. Finally, health loses stability through a transcritical bifurcation at $k_{pg} = 1.5$. The stable branch that is created corresponds to negative levels of pathogen and activated phagocytes and is therefore not included in the bifurcation figure. In summary, for $1.187 < k_{pg} < 1.5$ and $C_A = 0.2$, this

Fig. 2. Bifurcation diagrams and nullclines for the N^*/P subsystem. (a) Bifurcation diagram generated for $C_A = 0.2$ with bifurcation parameter k_{pg} . There is a saddle-node bifurcation at $k_{pg} = 0.8829$, Hopf bifurcation at $k_{pg} = 1.187$, where the system becomes bistable between septic death and health, and a transcritical bifurcation at $k_{pg} = 1.5$, where health loses stability. The stable branch emerging from the transcritical point corresponds to negative pathogen and activated phagocytes, a non-physiological situation not displayed. The number of bold curves a vertical line intersects corresponds to the number of stable outcomes possible for the parameter value represented by this line. Which asymptotic outcome is reached depends on the initial conditions of the system. For example, a vertical line at $k_{pg} = 1.3$ would intersect two bold curves; therefore, at this parameter value there are two stable outcomes, health and septic death. (b) Two-parameter bifurcation diagram. We follow the existence of stable septic death (the bold line) and the transcritical (dashed line) from (a), with C_A as the second parameter. This divides the $k_{pg}-C_A$ plane into regions labeled by the set of stable outcomes that exist. In the shaded region there are no stable fixed points and the system oscillates. The diamond represents the point where the bifurcation giving rise to stable septic death changes from a Hopf (below the diamond) to a saddle-node bifurcation (above the diamond). (c) Plot of the solid curve from (b) in (N^*, k_{pg}) space shows the level of activated phagocytes reached at the onset of stable septic death as a function of k_{pg} . Both N^* and k_{pg} decrease as C_A increases and again a diamond marks the change from a Hopf bifurcation (above the diamond) to a saddle-node bifurcation (below the diamond). (d), (e) Plots of the nullclines for this subsystem with $C_A = 0.2$ and $k_{pg} = 1.25$. The system is bistable between the health and septic death fixed points with a saddle point separating them. The unstable and stable manifolds of the saddle point are included in (d) and by zooming in on the boxed region, we see in (e) that the P -axis is divided into three regions by the P -nullcline and the stable manifold of the saddle point.

subsystem features bistability between health and septic death.

This bifurcation structure remains qualitatively similar for nearby values of C_A , while for sufficiently elevated C_A levels, septic death is stable as soon as it appears and we no longer observe a Hopf bifurcation. We examined the criteria for existence of stable septic death in a two-parameter bifurcation k_{pg} - C_A plane. A curve divides the plane in two regions (solid curve in Fig. 2(b)). For

parameter values on the left of the curve, stable septic death does not exist, while on the right, it does. Also in Fig. 2(b), at $k_{pg} = 1.5$, there is a dashed vertical line that denotes where the health state loses stability. This line further divides the plane, creating a total of four regions: health, health/septic death, septic death, and a shaded region. The first three regions are labeled by the stable states that corresponding parameter values support. In the shaded region, septic death does not exist, and health is



unstable. Therefore, there is no stable fixed point and trajectories oscillate. This does not represent a biologically observed state; however, once we combine subsystems below, oscillations will no longer occur.

In Fig. 2(c), we see the effect of C_A on the level of activated phagocytes (N^*) in the septic death state when it first becomes stable. From Fig. 2(b), we know that as C_A increases, the k_{pg} value at which the stable septic death state appears decreases. Biologically, this corresponds to a prediction that holding C_A at a larger constant level induces a greater inhibition of the immune response, allowing a less virulent pathogen to induce a septic death outcome. In theory, this inhibition of N^* could allow an initial enhancement of the build-up of P , which would subsequently evoke a large rise in N^* , leading to a high N^* septic death state; alternatively, the combination of higher C_A and low k_{pg} could suppress the level of N^* seen in septic death. Fig. 2(c) shows that in fact the latter possibility occurs, such that the activated phagocyte levels reached in septic death decrease, along with the pathogen growth rate, as the anti-inflammatory response increases.

For parameters corresponding to the region of septic death/health in Fig. 2(b), the N^*/P subsystem is bistable. As noted above, a saddle separatrix, specifically the stable manifold of a saddle fixed point, separates the two stable states, as we see Fig. 2(d) and (e) for $C_A = 0.2$. Notice the boxed region in Fig. 2(d). Zooming in on this region, as in Fig. 2(e), we see that the P nullcline and the stable manifold of the saddle point divide the P -axis into three regions. Suppose an initial pathogen load, P_0 , is introduced to the system, which had previously been in the health state. When P_0 falls in the first region, to the left of the P nullcline, the non-specific local response is able to eliminate the pathogen without any transient pathogen growth. If P_0 falls in the middle region, between the P nullcline and the stable manifold, then the pathogen is able to overcome the local response and initially grow before the activated phagocytes respond and clear the infection. If P_0 is in the final region, to the right of the stable manifold, then the immune response is unable to heal the individual. When the subsystems are combined, and the anti-inflammatory mediator is allowed to evolve dynamically, we shall see that these regions persist, with qualitatively similar properties. Thus, this analysis of the N^*/P system with a constant anti-inflammatory mediator is helpful in understanding the role of the activated phagocytes in the pro-inflammatory response to pathogen.

2.3. The N^*/D subsystem

When activated phagocytes respond to an infection, their presence in the tissue not only kills pathogens, but may also lead to collateral tissue damage (Goris et al., 1985; Takala et al., 1999). Damaged tissue releases pro-inflammatory cytokines, which causes further phagocyte activation. This positive feedback interaction between phagocytes and damage also exists in the absence of pathogen and can be

triggered by other stimuli, such as tissue trauma. Therefore, the N^*/D system should be bistable between health and aseptic death over a range of the anti-inflammatory mediator. Modeling the interactions between activated phagocytes and damage, we developed the N^*/D subsystem, which consists of the following:

$$\frac{dN^*}{dt} = \frac{s_{nr}R_2}{\mu_{nr} + R_2} - \mu_n N^*, \quad (4)$$

$$\frac{dD}{dt} = k_{dn}f_s(N^*) - \mu_d D, \quad (5)$$

where $R_2 = k_{nn}N^* + k_{nd}D$ and the saturation function is phenomenologically defined as $f_s(V) = V^6/(x_{dn}^6 + V^6)$.

As in the N^*/P systems (2) and (3), the activated phagocyte equation in the N^*/D system is derived by first considering a system of equations that includes the resting phagocytes and subsequently assuming that the resting phagocytes are in quasi-steady state. The only difference between the N^* equations (3) and (4) appears in the activation of resting phagocytes, which we now take to be affected by D rather than P . Correspondingly, R_1 from Eq. (3) is replaced by $R_2 = k_{nn}N^* + k_{nd}D$ in Eq. (4).

At low counts, activated phagocytes do not cause significant damage. However, as they accumulate in response to an infection, the activated phagocytes will cause tissue damage to accrue. Finally, once levels of activated phagocytes are sufficiently high, damage saturates, such that the activation of additional phagocytes has little impact on damage creation. We model this non-linearity in the induction of damage by activated phagocytes via the Hill-type function, f_s , in Eq. (5). The coefficient in f_s must be chosen to be sufficiently large to produce a reasonable basin of attraction for health in the N^*/D system (see Supplementary Materials for further explanation). We subtract the term $\mu_d D$ in Eq. (5) to represent tissue repair, resolution, and regeneration. Linear stability analysis of the health state, $(N^*, D) = (0, 0)$, shows that the eigenvalues are negative for $\mu_n > s_{nr}k_{nn}/\mu_{nr}$, which is the same condition that arose for the N^*/P subsystem and always holds for our baseline parameter set.

As in the N^*/P subsystem, we introduce the anti-inflammatory mediator (C_A) into the N^*/D subsystem as a parameter to ensure that our other parameter choices give the desired bistability for all physiological levels of C_A . As in the previous subsystem, the inclusion of the anti-inflammatory mediator leads to inhibition of activated phagocytes by two means. Specifically, the activation process itself is inhibited, which we model by replacing R_2 with $f(R_2)$ in Eq. (4), where f is the same saturating function defined for inhibition in the N^*/P subsystem. The ability of activated phagocytes to cause damage is also inhibited by the anti-inflammatory mediator, which we model by replacing N^* with $f(N^*)$ in Eq. (5).

As in the N^*/P subsystem, the nullclines of the modified N^*/D subsystem intersect such that there are two stable fixed points separated by a saddle node for appropriate

values of C_A . Similar to Fig. 2(d) and (e), Fig. 3(a) shows the nullclines and invariant sets of the N^*/D subsystem with $C_A = 0.2$. The stable manifold of the saddle point defines the threshold between health and aseptic death. The parameters and the Hill coefficient are chosen so that this threshold allows activated phagocytes to adequately respond to an inoculum of pathogen without triggering aseptic death.

In the bifurcation diagram for the anti-inflammatory mediator in Fig. 3(b), we see that the N^*/D subsystem displays bistability between health and aseptic death for $C_A < 0.626$. Note that as the level of C_A increases, the level

of activated phagocytes reached at aseptic death is decreased. This trend makes sense, since the anti-inflammatory mediator inhibits the activation of phagocytes. Eventually, this inhibition prevents the system from equilibrating at a state where N^* remains elevated; specifically, as C_A increases, the nullclines pull apart and eventually do not intersect. This occurs at the saddle node $C_A = 0.626$ and causes this subsystem to lose bistability. We note that this value lies above the physiological relevant range for C_A and also is consistent with the intuition that high C_A levels prevent the explosion of N^* needed for aseptic death.

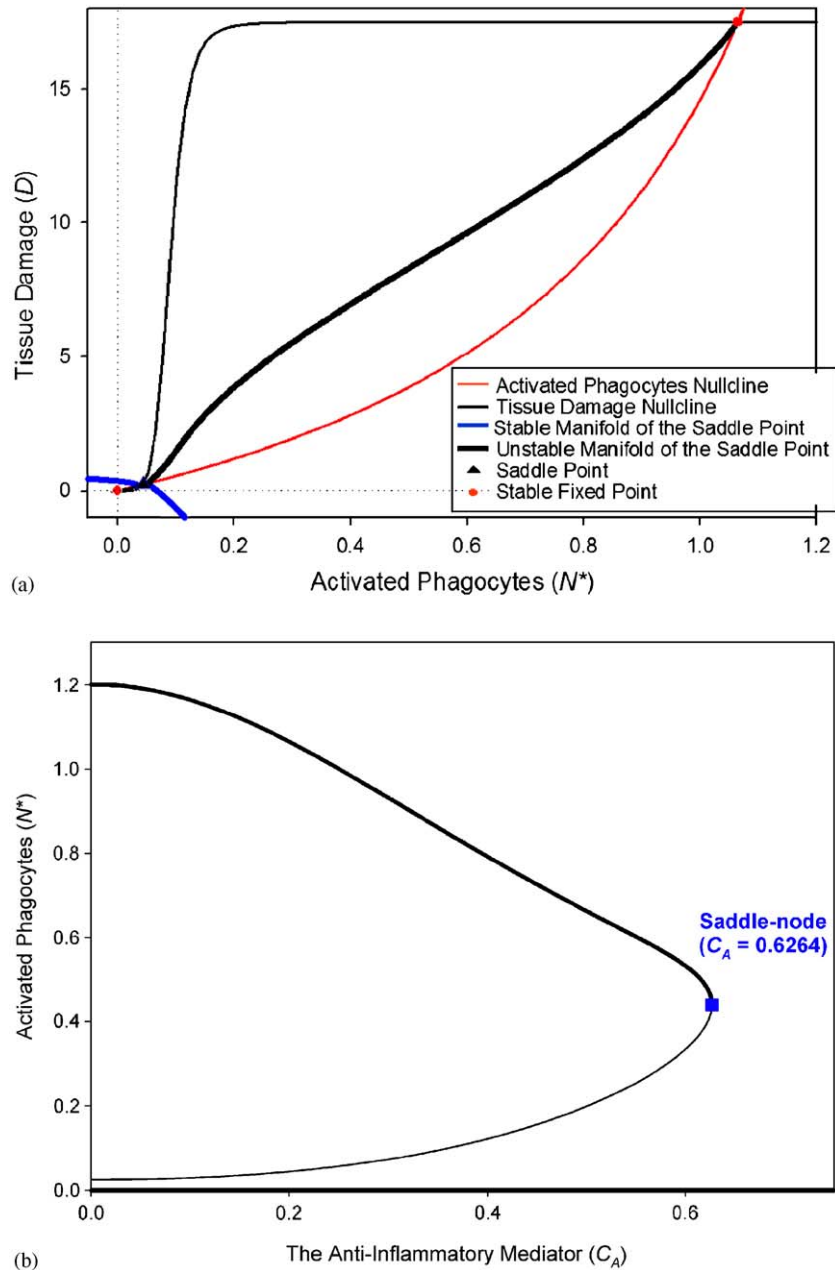


Fig. 3. Nullclines and bifurcation diagrams for the N^*/D subsystem. (a) Plot of the nullclines shows that the stable health and aseptic death fixed points are separated by a saddle point. The stable and unstable manifolds of the saddle point also are included. (b) Bifurcation diagram with bifurcation parameter C_A , showing bistability between health and aseptic death that is lost through a saddle-node bifurcation as C_A increases through 0.6264.

2.4. The three-variable subsystem

We combine the above two systems by including effects of both pathogen and damage on the rate at which the resting phagocytes are activated. To do this, we let $R_3 = k_{nm}N^* + k_{np}P + k_{nd}D$ and again assume that the resting phagocytes are in quasi-steady state to obtain the system of equations:

$$\frac{dP}{dt} = k_{pg}P \left(1 - \frac{P}{p_\infty}\right) - \frac{k_{pm}s_m P}{\mu_m + k_{mp}P} - k_{pn}N^*P, \quad (6)$$

$$\frac{dN^*}{dt} = \frac{s_{nr}R_3}{\mu_{nr} + R_3} - \mu_n N^*, \quad (7)$$

$$\frac{dD}{dt} = k_{df}s(N^*) - \mu_d D, \quad (8)$$

where

$$R_3 = k_{nm}N^* + k_{np}P + k_{nd}D$$

and

$$f_s(V) = \frac{V^6}{(x_{dn}^6 + V^6)}.$$

Models (6)–(8) exhibit the combined dynamics of the previous two subsystems. The conditions for stable health are unchanged from the N^*/P subsystem, since $D = 0$ at the health fixed point. In particular, health is stable for low pathogen growth rate (k_{pg}), but loses stability at a transcritical bifurcation at $k_{pg} = 1.5$ as k_{pg} is increased. Since this instability is induced by the pathogen dynamics, it follows that even after this stability loss, the healthy state retains a two-dimensional stable manifold, such that small perturbations in the non-pathogen components lead to healthy resolutions. For low or moderate growth rate, the system inherits the existence of stable aseptc death from the bistability of the N^*/D subsystem. Consequently, for low pathogen growth rate, the physiological outcomes after pathogenic infection are health, achieved when the initial pathogen level is low, and aseptc death, arising when the initial inoculum of pathogen is large enough that the resulting phagocytic response results in large tissue damage.

As in the N^*/P subsystem, increasing pathogen growth rate leads to a bifurcation that introduces the possibility of septic death. Fig. 4(a) shows a bifurcation diagram with $C_A = 0.2$, in which we see that this bifurcation is a Hopf at $k_{pg} = 1.707$. This diagram also shows the transcritical bifurcation that destabilizes the health state at $k_{pg} = 1.5$; the second branch of equilibria participating in this bifurcation is not shown, since it corresponds to a non-physiological state with negative pathogen and activated phagocytes. Since health is already unstable for $k_{pg} < 1.707$, there are only two possible stable outcomes, aseptc death and septic death, until $k_{pg} = 2.769$, when aseptc death loses stability through a second transcritical bifurcation. Aseptc death loses stability when k_{pg} becomes so large that

the immune system cannot clear the pathogen, preventing stability of a state with a non-zero pathogen level and leaving septic death as the only stable state for the system.

Despite the bistability between aseptc and septic death for $1.707 < k_{pg} < 2.769$, initial conditions with only pathogen elevated, and all other variables at healthy levels, always lead to septic death for fixed C_A . The aseptc death outcome is attainable if tissue trauma ($D_0 > 0$) occurs in the absence of pathogen or if the initial level of activated phagocytes ($N^*_0 > 0$) is elevated (with or without pathogen). A pre-activated immune system allows the infection to be cleared, avoiding septic death. However, activated phagocytes continue to be elevated in response to the pathogen, and this triggers aseptc death.

Next, we follow the bifurcation points in a two-parameter bifurcation diagram in the k_{pg} – C_A plane (Fig. 4(a) and (b)). The existence of septic death is represented by the solid curve. For a combination of parameters on the right of this curve, this system enters septic death (given a sufficient inocula for pathogen), while on the left, septic death does not exist. The transcritical bifurcation where health loses stability is represented by the vertical dashed line at $k_{pg} = 1.5$. To the right of this line the health state is unstable. The transcritical threshold corresponding to the loss of stability of aseptc death is represented by a blue dashed curve. Also, for C_A levels above the horizontal, dashed line, aseptc death does not exist due to the same saddle-node bifurcation we showed in the N^*/D subsystem. Therefore, aseptc death is not a possible outcome above the horizontal, dashed line or to the right of the blue dashed curve. Combining these bifurcation structures we are able to label each region, as we did in Fig. 2(b), by the stable states they support.

From the two-parameter bifurcation diagram in Fig. 4(b), we observe that for $C_A > 0.234$, the bifurcation giving rise to the existence of septic death occurs at a $k_{pg} < 1.5$. Therefore, if $0.234 < C_A < 0.626$ (indicated by the horizontal, dashed line in Fig. 4(b)), there is a range of k_{pg} for which all three outcomes are stable. As in the case with $C_A = 0.2$ and bistability between aseptc and septic death, the path to aseptc death is sensitive to initial conditions and there is a propensity to enter septic death when only pathogen is initially introduced.

2.5. The four-variable model

We complete the model derivation by introducing time dependence to the anti-inflammatory mediator C_A , thereby obtaining our four-variable reduced model of the acute immune response. The production of the anti-inflammatory mediator is associated with the presence of activated phagocytes (de Waal et al., 1991) and elevated markers of tissue damage (Stvrtnova et al., 1995). As discussed in the development of the various subsystems considered above, the anti-inflammatory mediator (C_A) regulates the immune response by inhibiting the production and effects of activated phagocytes and damage. More specifically, the

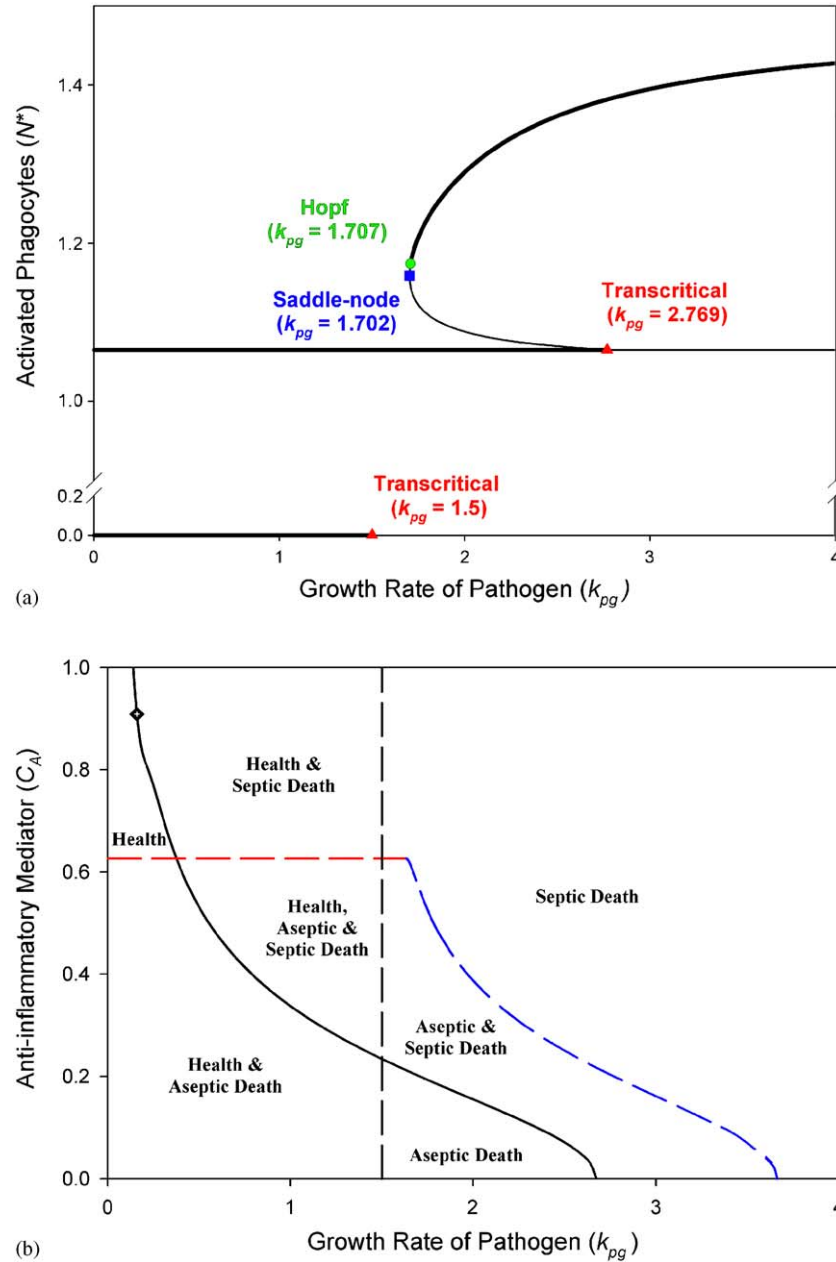


Fig. 4. Bifurcation diagrams for the three-variable subsystem. (a) Bifurcation diagram for k_{pg} with $C_A = 0.2$. Health and aseptic death both lose stability through transcritical bifurcations, at $k_{pg} = 1.5$ and 2.769 , respectively. The emerging stable states correspond to non-physiological states and are not shown. At $k_{pg} = 1.702$ there is a saddle-node bifurcation giving rise to two additional fixed points that are both initially unstable. However, at $k_{pg} = 1.707$, a Hopf bifurcation creates a stable state, which corresponds to septic death. Therefore, when $k_{pg} < 1.5$, there is bistability between health and aseptic death; for $1.5 < k_{pg} < 1.707$, aseptic death is the only stable state; there is bistability between aseptic and septic death for $1.707 < k_{pg} < 2.769$; and septic death is the only stable state for $k_{pg} > 2.769$. (b) Two-parameter bifurcation diagram generated by following the Hopf, saddle node, and transcritical bifurcations from (a). The black solid curve represents the onset of stable septic death. The diamond again represents the switch from a Hopf (below) to a saddle node (above) bifurcation. Each region is labeled by the possible stable outcomes in the corresponding parameter regime. Transcritical bifurcations are represented by dashed curves; the vertical is the loss of stable health and the blue the loss of stable aseptic death. The red, dashed, horizontal line corresponds to where the aseptic death state loses existence due to a saddle-node bifurcation as C_A is increased, which is related to the saddle point seen in Fig. 3(b) from the N^*/D subsystem.

presence of C_A decreases the ability of activated phagocytes to react to other cell types, reducing their effectiveness against the pathogen, their induction of damage, and their production of additional C_A (de Waal et al., 1991). The recruitment of C_A by tissue damage (D) is similarly

inhibited. Further, C_A compromises all means of activation of resting phagocytes.

As in the various subsystems, inhibition of activated phagocytes by the anti-inflammatory mediator (C_A) is incorporated in the model by replacing N^* with $f(N^*) =$

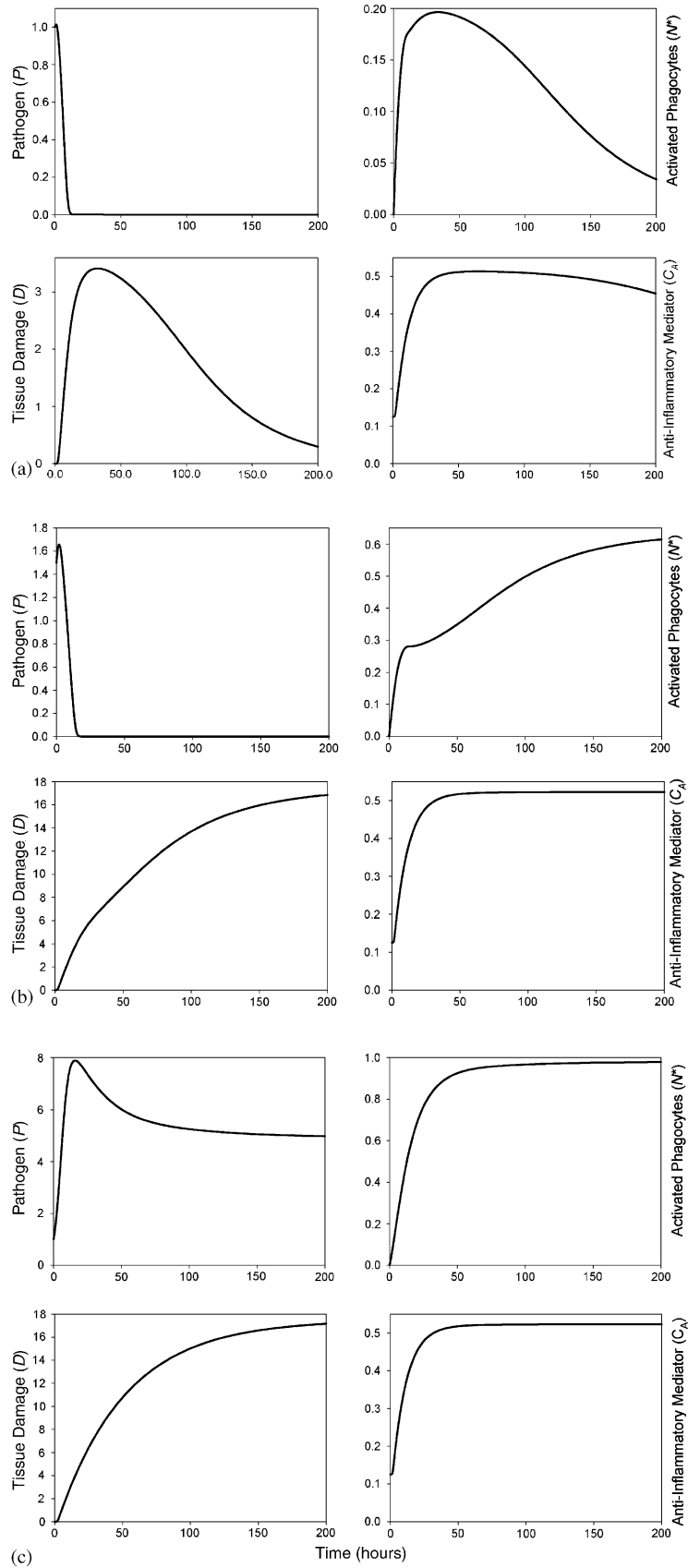


Fig. 5. Transients from the evolution of the reduced model. (a) Healthy outcome, with $k_{pg} = 0.3/\text{h}$ and initial conditions $P = 1$, $N^* = 0$, $D = 0$, and $C_A = 0.125$. (b) Aseptic death, with $k_{pg} = 0.3$ and initial conditions $P = 1.5$, $N^* = 0$, $D = 0$, and $C_A = 0.125$. (c) Septic death, with $k_{pg} = 0.6$, such that septic death is a possible outcome, and initial conditions $P = 1$, $N^* = 0$, $D = 0$, and $C_A = 0.125$.

$N^*/(1 + (C_A/c_\infty)^2)$ in Eqs. (6) and (8). The inhibition of the activation of resting phagocytes is modeled by replacing R_3 with $R = f(R_3) = f(k_{nm}N^* + k_{np}P + k_{nd}D)$. Note that f limits to zero as C_A approaches infinity, and therefore if C_A levels are manipulated to be sufficiently high (above the maximum reached in response to an infection), then they will correspond to nearly complete inhibition of immune activation, which is experimentally observed (D'Andrea et al., 1993).

The C_A equation contains a source of C_A , denoted s_c , and a term modeling the production of anti-inflammatory mediator from damage and activated phagocytes, which takes the form $k_{cn}(N^* + k_{cnd}D)/(1 + N^* + k_{cnd}D)$, before inhibition is incorporated. This expression is a Michaelis–Menten-type term, in which k_{cnd} controls the effectiveness of damage, relative to activated phagocytes, in producing C_A . Including inhibition in this term, we obtain $k_{cn}f(N^* + k_{cnd}D)/(1 + f(N^* + k_{cnd}D))$.

Finally, incorporating these changes and additions into our three-variable model, Eqs. (6)–(8) result in our four-variable model, which consists of the following:

$$\frac{dP}{dt} = k_{pg}P \left(1 - \frac{P}{P_\infty}\right) - \frac{k_{pm}s_m P}{\mu_m + k_{mp}P} - k_{pn}f(N^*)P, \quad (9)$$

$$\frac{dN^*}{dt} = \frac{s_{nr}R}{\mu_{nr} + R} - \mu_n N^*, \quad (10)$$

$$\frac{dD}{dt} = k_{dn}f_s(f(N^*)) - \mu_d D, \quad (11)$$

$$\frac{dC_A}{dt} = s_c + \frac{k_{cn}f(N^* + k_{cnd}D)}{1 + f(N^* + k_{cnd}D)} - \mu_c C_A, \quad (12)$$

where

$$R = f(k_{nm}N^* + k_{np}P + k_{nd}D),$$

$$f(V) = V/(1 + (C_A/c_\infty)^2),$$

and

$$f_s(V) = V^6/(x_{dn}^6 + V^6).$$

We shall refer to Eqs. (9)–(12) as the *reduced model*, because it describes a highly abstracted representation of the complexity of the acute immune response. The XPPAUT code for the reduced model and all subsystems is included with the Supplementary Materials.

3. Results

The reduced model, Eqs. (9)–(12), exhibits the same physiological fixed points as discussed above for the three-variable model. The health state is a fixed point with $P = 0$, $N^* = 0$, $D = 0$, and $C_A = s_c/\mu_c$. The anti-inflammatory mediator is non-zero in this state, corresponding to the background level of these cytokines that exists in healthy individuals. In aseptc death, $P = 0$, but N^* , D , and C_A are non-zero. All variables are non-zero in septic death. Model dynamics for initial conditions leading to health, or aseptc

and septic death are depicted in Fig. 5(a), (b), and (c), respectively. The qualitative dependence of the existence of stable states on the pathogen growth rate k_{pg} is maintained as in the three-variable model. As k_{pg} is increased, the septic death state comes into existence via a Saddle-node bifurcation at $k_{pg} = 0.5137$ and the aseptc death state loses stability at $k_{pg} = 1.755$, as can be seen in the bifurcation graph presented in Fig. 6. As in the subsystems, health loses stability at a transcritical bifurcation at $k_{pg} = 1.5$. The second branch of equilibria involved in this transcritical bifurcation corresponds to a non-physiological state and is not included in Fig. 6.

Utilizing both the three-variable subsystem, with the anti-inflammatory mediator treated as a parameter, and the reduced model, we explore several aspects of the role of C_A : (1) we investigate the effects of allowing C_A to dynamically depend on other model variables, which we compare to results found by holding the anti-inflammatory response at various constant levels, (2) we vary parameters that govern the speed of the anti-inflammatory response, (3) we analyse the effects resulting from the presence of initially elevated or depleted C_A levels when an infection is introduced, and (4) we consider the effects of reducing or elevating (resetting) C_A after an infection has progressed for multiple hours and then allowing the full model to evolve, a manipulation that simulates a therapeutic intervention with an anti-inflammatory mediator.

We first ask whether the dynamics of the anti-inflammatory response are important, or whether a similar protection against runaway inflammation is achieved by the inclusion of a constant presence of the anti-inflammatory mediator in the model. In Fig. 7, we compare the

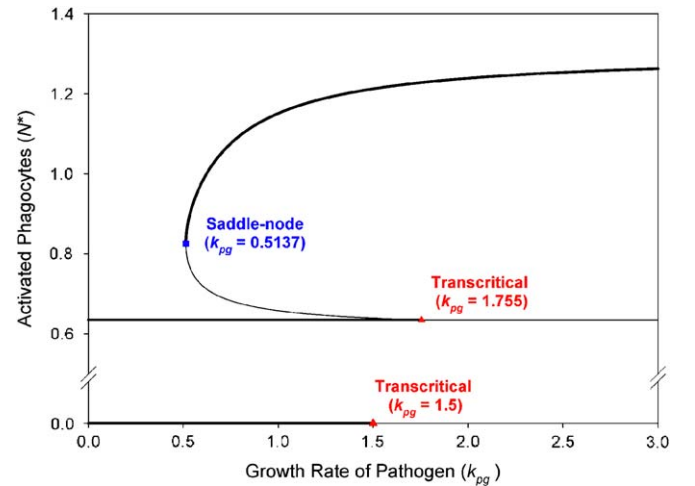


Fig. 6. Bifurcation diagram for the four-variable reduced model. Septic death comes into existence via a saddle-node bifurcation at $k_{pg} = 0.5137/h$. Health and aseptc death lose stability by transcritical bifurcations at $k_{pg} = 1.5$ and 1.755 , respectively. As in the subsystems, the emerging stable states are not shown, since they are non-physiological. For $k_{pg} < 0.5137$, the model is bistable between health and aseptc death. The model has all three states stable for $0.5137 < k_{pg} < 1.5$. There is bistability between aseptc and septic death for $1.5 < k_{pg} < 1.755$. Finally, above $k_{pg} = 1.755$, the only stable state is septic death.

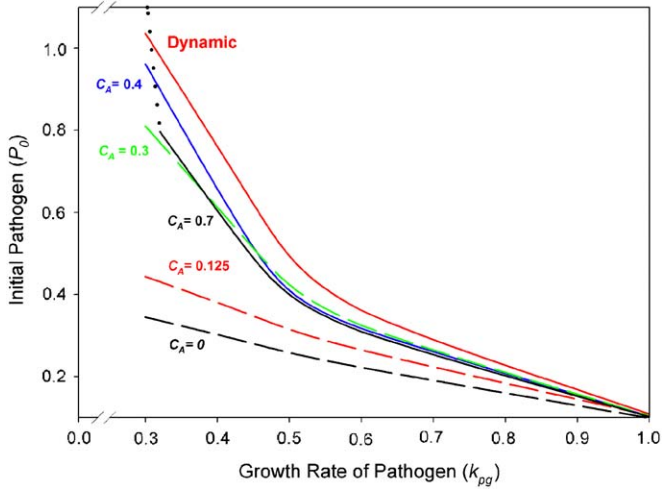


Fig. 7. The basin of attraction for the health state depends on C_A . For each constant C_A level shown, the three-variable subsystem was used to determine the level of initial pathogen that is the threshold between health and death (aseptic or septic), over a range of k_{pg} . Using the reduced model, with initial conditions $N^* = 0$, $D = 0$, and $C_A = 0.125$ and with dynamic C_A , the same was done, giving rise to the curve labeled “Dynamic”. The dotted portion of the $C_A = 0.7$ curve (black) represents a range of k_{pg} where health is the only stable outcome.

outcomes associated with a dynamic C_A response with those found with a variety of constant levels of C_A . At different k_{pg} values, we determine the level of initial pathogen that is the threshold between health and death (aseptic or septic). The curve associated with $C_A = 0$ lies below all other curves; the presence of the anti-inflammatory mediator, whether dynamic or constant, allows a larger initial pathogen load or growth rate to be tolerated over all physiological (>0) values of the pathogen growth rate, k_{pg} . An interesting result arising from simulation of the reduced model is that a dynamic anti-inflammatory mediator is almost always more effective than constant levels of the anti-inflammatory mediator at producing a healthy outcome following infection. Indeed, the curve associated with dynamic C_A in Fig. 7 is above all other curves for most k_{pg} levels. The only exception is that at low growth rate ($k_{pg} < 0.307$), the curve for $C_A = 0.7$ (very high C_A) ends and is continued by a dotted line, which crosses above the curve for dynamic C_A . In this region, with $C_A = 0.7$, the only outcome is health, and hence the threshold between health and death is no longer defined. For infections of such low virulence, even large anti-inflammatory levels will not thwart inflammation to a degree that allows runaway infection and death. Teleologically, our model demonstrates that a dynamic anti-inflammatory response increases the robustness of the immune response to infection, allowing the body to recover over a broad range of pathogen growth rate, yet in a way that minimizes life-threatening tissue damage.

Given that a dynamic anti-inflammatory response is advantageous, we now consider how the rate of this response affects the overall outcome following infection.

Considering a trajectory that is in the basin of attraction of health but close to the threshold between health and death, we altered the time-scale of C_A by modifying the rate constants reflecting the production (k_{cn}) and decay rate (μ_c) of the anti-inflammatory mediator simultaneously. A slight increase in these rates helped the system to restore health sooner, but larger increases favored septic death. On the other hand, slowing down the anti-inflammatory dynamics causes the trajectory to proceed to aseptic death. Similar results are obtained over a broad range of pathogen growth rates.

Next, we use the reduced model to explore the impact of baseline anti-inflammatory mediator levels on response to infection. First, we vary the initial level of C_A (C_{A0}) for a given initial level of pathogen (P_0) and determine the threshold between health and death at this P_0 . This was repeated for multiple values of P_0 at fixed k_{pg} values. As depicted in Fig. 8, this process defines, for each k_{pg} value, a boundary between health and death illustrated by the corresponding curve. Because the local non-specific immune response in our model is not inhibited by C_A , the threshold between health and death cannot fall below the level of pathogen that the local response is capable of clearing, regardless of the initial levels C_A . Thus, a vertical asymptote, close to the $k_{pg} = 1$ curve, is reached for large k_{pg} . The dotted line in Fig. 8 indicates the level of C_{A0} found in the healthy state (background), call it C_{A0}^* . From Fig. 8, we see that the effect of C_{A0} is generally stronger at lower k_{pg} . For such k_{pg} , a reduction in C_{A0} from C_{A0}^* moves the threshold for death to lower P_0 . Conversely, increasing C_{A0} allows the system to handle higher P_0 . However, the changes that occur for higher k_{pg} , while milder, are opposite to these. Moreover, even for low k_{pg} , the

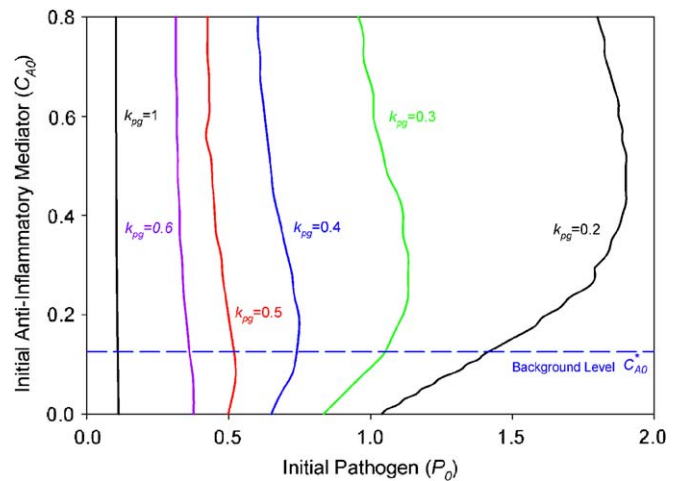


Fig. 8. The threshold between health and death depends on the initial anti-inflammatory mediator and pathogen levels in the reduced model. At each k_{pg} value indicated we find the initial C_A level that is the threshold between health and death outcomes, given that N^* and D are initially at their baseline (zero) levels. Initial conditions to the left of each curve lead to health while those to the right give rise to either septic or aseptic death. The baseline level of C_A , corresponding to health in the reduced model, is indicated by the blue dashed line.

threshold for death shifts back to lower P_0 when C_{A0} is made sufficiently large. Indeed, it appears that the background C_A level, C_{A0}^* , is fairly optimally situated to allow for maximal or near-maximal threshold P_0 for a fairly broad range of high pathogen growth rates values, without undue compromise of protection at lower k_{pg} . Interestingly, however, this background level is not globally optimal.

For solutions to the reduced model with initial conditions in the basin of attraction of the health state, C_A returns to baseline significantly later than all other variables (Fig. 5(a)). Therefore, after an infection is cleared, there is a period of time when only C_A is elevated, a window of relative immune suppression. Fig. 8 allows us to consider the effects of introducing a second infection during this window. Although for high k_{pg} , the baseline level of C_A leads to a larger basin of attraction for health than does elevated C_A , the elevated levels of C_A found immediately after an infection are only mildly detrimental. At these levels, C_A offers significant protection against a subsequent infection of a low or moderate k_{pg} (see also Day et al., 2006).

Multiple clinical trials have been conducted in which an anti-inflammatory mediator is administered as treatment to individuals with severe clinical sepsis (i.e. typically a highly inflamed state), where death is a frequent outcome (Annane, 2001; Marshall, 2000). To mimic treatment aimed at modulating the anti-inflammatory mediator after an initial infection, we devised an in silico experiment where an initial pathogen is injected into the reduced model, Eqs. (9)–(12). The infection is allowed to evolve for several hours at which point we instantly decrease or increase the level of C_A , to simulate a therapeutic intervention aimed at depleting or raising the availability of C_A . The simulation then proceeds according to Eqs. (9)–(12). Initially, we ran simulations where the intervention was performed at 8, 10, and 12 h after pathogen injection. The results depicted in Fig. 9, obtained for the 10-h intervention, are representative of the case with moderate pathogen growth rate, where the simulation still results in health restoration, yet the solution lies near the threshold between health and aseptic death. In Fig. 9, a sufficiently small depletion of C_A (e.g. $C_A = 0.24$) still yields a healthy outcome, but resolution to health takes longer. More substantial depletion of C_A (e.g. $C_A = 0-0.2$) pushes the system to aseptic death; activated phagocytes clear the infection successfully yet are insufficiently inhibited, such that persistent collateral tissue damage results. If instead C_A values are instantly raised beyond 0.35, the simulation leads to septic death due to an excessive inhibition of activated phagocytes, which cannot mount a substantial attack on the pathogen. Therefore, over the time window explored, a modest increase in the anti-inflammatory mediator may indeed be slightly beneficial (e.g. $C_A = 0.32$ in Fig. 9), but it is important to prevent an overly large increase. This finding could be particularly crucial in clinical circumstances where the body cannot mount a sufficient anti-inflammatory response

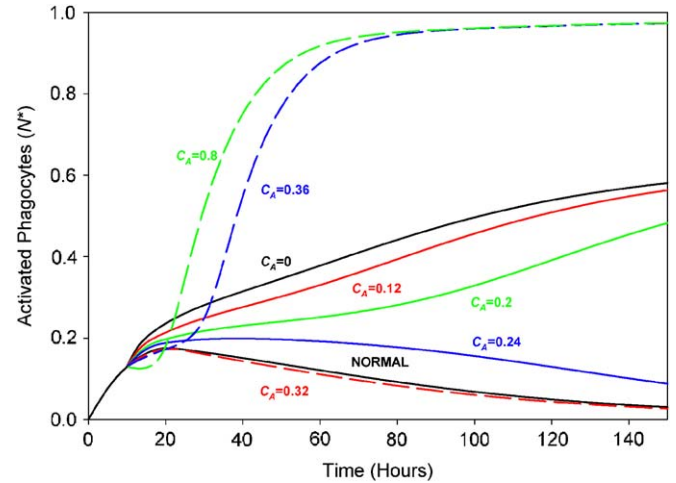


Fig. 9. Altering the anti-inflammatory mediator levels after an infection has progressed can dramatically alter outcome. In this example, we allow an infection, triggered by an initial pathogen injection of 0.36 with $k_{pg} = 0.6/h$, to progress for 10 h. After this, the anti-inflammatory mediator (C_A) is increased (dashed lines) or decreased (solid lines) without altering pathogen, activated phagocytes, and damage levels. The curve labeled “NORMAL” is the time course obtained without manipulation of the C_A level from its normal level of 0.303, and all other curves are labeled by their adjusted C_A levels, as introduced at 10 h.

(Annane, 2001; Annane et al., 2002). In such situations, a modest transient increase in anti-inflammation mediator would change the outcome from aseptic death to health, but larger increases would be problematic.

Finally, we explored the sensitivity of these results to pathogen growth rate and timing of intervention. For larger k_{pg} , the thresholds between health, aseptic death, and septic death are quite close together. As we raise k_{pg} from the example in Fig. 9, we find that interventions featuring significant increases in C_A continue to promote septic death, while significant decreases favor aseptic death. However, for sufficiently large k_{pg} , aseptic death becomes less of a threat, while there is a propensity for a pathogenic explosion leading to septic death. In these cases, the removal of most or all of the C_A present at the time of intervention is optimal for yielding a return to health. We note that if the delay before intervention is increased for moderate k_{pg} , then a greater C_A input is needed to avoid aseptic death, since N^* builds up during the time before intervention. In cases of high k_{pg} , excessive delays before removal of C_A can eliminate their ameliorative effects by prolonging the period of insufficiently restrained pathogen growth. These results highlight further that the outcome of anti-inflammatory therapy will be highly sensitive to the nature of the infection being treated and the details of the therapeutic protocol.

4. Discussion

We have derived a reduced model of the acute inflammatory response to infection that includes an anti-inflammatory mediator. Simulation and bifurcation

analysis of this model suggest that anti-inflammation plays several important roles in the restoration of health. First, anti-inflammation expands the basin of attraction of health compared to that present in models lacking anti-inflammation (Kumar et al., 2004), which is a desirable feature, given that we expect health to be a robust state. Second, we demonstrate an advantage, in terms of healthy resolution of infection, conferred by the dynamic nature of the anti-inflammatory response, in comparison to a tonic response. This advantage holds in all situations except for the mildest of infections, which, in any case, do not present a vital threat. This is illustrated in current clinical practice, where distressing symptoms associated with mild infections are alleviated by the co-administration of antibiotics and anti-inflammatory mediators. The reduced model also underlines the importance of the different response rates of substances promoting inflammation, represented in the model by N^* , and of the anti-inflammatory mediator that limit this response. Specifically, our results suggest that these rates are fairly well tuned to optimize healthy outcomes to pathogenic infection. Further, we have used simulations of our model to explore how variations in levels of the anti-inflammatory mediator present initially or at some time after initial infection affect the restoration of health following an inflammatory response.

We followed a systematic, modular approach to model development, building our reduced model from subsystems, each one with biologically plausible dynamics. Indeed, by building up this model through modules, we gain a clear understanding of how each element and interaction in the system contributes to the overall network dynamics. We also ensure that the final model behaves in a way that is consistent with situations in which particular features are absent, such as tissue damage without pathogen exposure, or are experimentally manipulated.

Our results illustrate the point that administration of an anti-inflammatory mediator during the response to an infection may compromise outcome (Fig. 9). The administration of pharmacological doses of steroids, which are potent natural anti-inflammatory mediators, in severely septic patients, has clearly resulted in worse survival (Schumer, 1976; Sprung et al., 1984). This situation corresponds in our model to either the maintenance of tonic elevated levels of the anti-inflammatory mediator or the transient administration of the anti-inflammatory mediator, in patients who would otherwise survive or evolve to aseptic death, causing septic death (Fig. 9). The association between significant immune suppression and infectious complications is clearly an ongoing concern for several groups of patients. Fortunately, the anti-inflammatory mediator, in addition to being conducive to the healing phase of injury, also plays a role in the acute phase of infection as well. A significant body of recent evidence suggests that low-dose immunosuppression with an anti-inflammatory mediator may in fact improve outcome in patients with severe infection, particularly in patients with an insufficient anti-inflammatory response (Annane, 2001;

Annane et al., 2002). Our simulations highlight the dependence of the outcomes of such interventions on pathogen virulence (Fig. 8) and timing of intervention, as discussed in the previous section. Therefore, studies such as those we have performed may be useful for subsequent investigations of anti-inflammatory therapeutic agents. For example, the only approved therapeutic agent for patients with severe sepsis, recombinant human activated Protein C, has anti-inflammatory properties (Bernard et al., 2001; Joyce and Grinnell, 2002; Nick et al., 2004) and the proper degree of modulation with this agent, alone or in combination with others, remains a very active focus of clinical research (Cross and Opal, 2003; Marshall, 2003). How the various features of the inflammatory response interact to govern the outcome following multiple insults, including pathogen, trauma, endotoxin, or other stimuli, also warrants intensive computational exploration (Day et al., 2006).

The biological relevance of our analysis and conclusions are limited by the significant oversimplification present in our reduced model and the difficulty in translating functions such as “pro-inflammation”, “anti-inflammation” and “damage” into measurable quantities. We are also involved with the development of a much larger model that directly addresses this limitation, where predictions are compared to prospectively collected experimental data (Chow et al., 2005). Such large-scale models, however, do not allow for detailed analysis, where emergent behaviors and drivers of such behavior are clearly identified and characterized. Future directions for study include a more detailed biological characterization of anti-inflammatory substances, since they differ widely in the time-scale and specificity of their activity, and a detailed mathematical analysis of the use of anti-inflammatory mediators as “therapeutic” agents, depending on time-scale as well as time and intensity of intervention. The experimental and clinical relevance of these efforts will continue to grow as methods are developed to better link reduced models and more complex models, both from top-down and bottom-up approaches.

Acknowledgments

This work was partial supported by NIH Award R01-GM67240.

Appendix A. Supplementary materials

Supplementary information associated with this article can be found in the online version at [doi:10.1016/j.jtbi.2006.02.016](https://doi.org/10.1016/j.jtbi.2006.02.016).

References

- Andersson, U., Wang, H., Palmblad, K., Aveberger, A.C., Bloom, O., Erlandsson-Harris, H., Janson, A., Kokkola, R., Zhang, M., Yang,

- H., Tracey, K.J., 2000. High mobility group 1 protein (HMG-1) stimulates proinflammatory cytokine synthesis in human monocytes. *J. Exp. Med.* 192, 565–570.
- Annane, D., 2001. Corticosteroids for septic shock. *Crit. Care Med.* 29, 117–120.
- Annane, D., Sebille, V., Charpentier, C., Bollaert, P.E., Francois, B., Korach, J.M., Capellier, G., Cohen, Y., Azoulay, E., Troche, G., Chaumet-Riffaut, P., Bellissant, E., 2002. Effect of treatment with low doses of hydrocortisone and fludrocortisone on mortality in patients with septic shock. *JAMA* 288, 862–871.
- Bacon, G.E., Kenny, F.M., Murdaugh, H.V., Richards, C., 1973. Prolonged serum half-life of cortisol in renal failure. *Johns Hopkins Med. J.* 132, 127–131.
- Bernard, G.R., Vincent, J.L., Laterre, P.F., LaRosa, S.P., Dhainaut, J.F., Lopez-Rodriguez, A., Steingrub, J.S., Garber, G.E., Helterbrand, J.D., Ely, E.W., Fisher Jr., C.J., 2001. Efficacy and safety of recombinant human activated protein C for severe sepsis. *N. Engl. J. Med.* 344, 699–709.
- Bocci, V., 1991. Interleukins. *Clinical pharmacokinetics and practical implications.* *Clin. Pharmacokinet.* 21, 274–284.
- Branwood, A., Noble, K., Schindhelm, K., 1992. Phagocytosis of carbon particles by macrophages in vitro. *Biomaterials* 19, 646–648.
- Chow, C.C., Clermont, G., Kumar, R., Lagoa, C., Tawadrous, Z., Gallo, D., Betten, B., Bartels, J., Constantine, G., Fink, M.P., Billiar, T.R., Vodovotz, Y., 2005. The acute inflammatory response in diverse shock states. *Shock* 24, 74–84.
- Coxon, A., Tang, T., Mayadas, T.N., 1999. Cytokine-activated endothelial cells delay neutrophil apoptosis in vitro and in vivo. A role for granulocyte/macrophage colony-stimulating factor. *J. Exp. Med.* 190, 923–934.
- Cross, A.S., Opal, S.M., 2003. A new paradigm for the treatment of sepsis: is it time to consider combination therapy? *Ann. Intern. Med.* 138, 502–505.
- D'Andrea, A., ste-Amezaga, M., Valiante, N.M., Ma, X., Kubin, M., Trinchieri, G., 1993. Interleukin 10 (IL-10) inhibits human lymphocyte interferon gamma-production by suppressing natural killer cell stimulatory factor/IL-12 synthesis in accessory cells. *J. Exp. Med.* 178, 1041–1048.
- Day, J., Rubin, J., Vodovotz, Y., Chow, C.C., Reynolds, A., Clermont, G., 2006. A reduced mathematical model of the acute inflammatory response II. Capturing scenarios of repeated endotoxin administration. *J. Theor. Biol.*, in press.
- de Waal, M.R., Abrams, J., Bennett, B., Figdor, C.G., de Vries, J.E., 1991. Interleukin 10(IL-10) inhibits cytokine synthesis by human monocytes: an autoregulatory role of IL-10 produced by monocytes. *J. Exp. Med.* 174, 1209–1220.
- Ermentrout, G.B., 2002. *Simulating, Analyzing, and Animating Dynamical Systems: A Guide to XPPAUT for Researchers and Students*, first ed. Society for Industrial & Applied Mathematics, Philadelphia.
- Fuchs, A.C., Granowitz, E.V., Shapiro, L., Vannier, E., Lonnemann, G., Angel, J.B., Kennedy, J.S., Rabson, A.R., Radwanski, E., Afrime, M.B., Cutler, D.L., Grint, P.C., Dinarello, C.A., 1996. Clinical, hematologic, and immunologic effects of interleukin-10 in humans. *J. Clin. Immunol.* 16, 291–303.
- Goris, R.J., te Boekhorst, T.P., Nuytinck, J.K., Gimbrere, J.S., 1985. Multiple-organ failure. Generalized autodestructive inflammation? *Arch. Surg.* 120, 1109–1115.
- Huhn, R.D., Radwanski, E., Gallo, J., Afrime, M.B., Sabo, R., Gonyo, G., Monge, A., Cutler, D.L., 1997. Pharmacodynamics of subcutaneous recombinant human interleukin-10 in healthy volunteers. *Clin. Pharmacol. Ther.* 62, 171–180.
- Isler, P., de Rochemonteix, B.G., Songeon, F., Boehringer, N., Nicod, L.P., 1999. Interleukin-12 production by human alveolar macrophages is controlled by the autocrine production of interleukin-10. *Am. J. Respir. Cell Mol. Biol.* 20, 270–278.
- Janeway Jr., C.A., Medzhitov, R., 2002. Innate immune recognition. *Annu. Rev. Immunol.* 20, 197–216.
- Janeway Jr., C.A., Travers, P., Walport, M., Shlomchik, M., 2001. *Immunobiology: The Immune System in Health and Disease*, fifth ed. Garland Publishing, New York.
- Joyce, D.E., Grinnell, B.W., 2002. Recombinant human activated protein C attenuates the inflammatory response in endothelium and monocytes by modulating nuclear factor-kappaB. *Crit. Care Med.* 30, S288–S293.
- Kumar, R., Clermont, G., Vodovotz, Y., Chow, C.C., 2004. The dynamics of acute inflammation. *J. Theor. Biol.* 230, 145–155.
- Marshall, J.C., 2000. Clinical trials of mediator-directed therapy in sepsis: what have we learned? *Intensive Care Med.* 26 (Suppl. 1), 75–83.
- Marshall, J.C., 2003. Such stuff as dreams are made on: mediator-directed therapy in sepsis. *Nat. Rev. Drug Discov.* 2, 391–405.
- Nick, J.A., Coldren, C.D., Geraci, M.W., Poch, K.R., Fouty, B.W., O'Brien, J., Gruber, M., Zarini, S., Murphy, R.C., Kuhn, K., Richter, D., Kast, K.R., Abraham, E., 2004. Recombinant human activated protein C reduces human endotoxin-induced pulmonary inflammation via inhibition of neutrophil chemotaxis. *Blood* 104 (13), 3878–3885.
- Ochsenbein, A.F., Zinkernagel, R.M., 2000. Natural antibodies and complement link innate and acquired immunity. *Immunol. Today*, 21, 624–630.
- Paulsen, F., Pufe, T., Conradi, L., Varoga, D., Tsokos, M., Papendieck, J., Petersen, W., 2002. Antimicrobial peptides are expressed and produced in healthy and inflamed human synovial membranes. *J. Pathol.* 198, 369–377.
- Raj, P.A., Dentino, A.R., 2002. Current status of defensins and their role in innate and adaptive immunity. *FEMS Microbiol. Lett.* 206, 9–18.
- Schumer, W., 1976. Steroids in the treatment of clinical septic shock. *Ann. Surg.* 184, 333–341.
- Spector, W.S. (Ed.), 1956. *Handbook of Biological Data*. W.B. Saunders Company, London.
- Sprung, C.L., Caralis, P.V., Marcial, E.H., Pierce, M., Gelbard, M.A., Long, W.M., Duncan, R.C., Tendler, M.D., Karpf, M., 1984. The effects of high-dose corticosteroids in patients with septic shock. A prospective, controlled study. *N. Engl. J. Med.* 311, 1137–1143.
- Strogatz, S.H., 1994. *Nonlinear Dynamics and Chaos: With Application to Physics, Biology, Chemistry, and Engineering*. Westview Press, Cambridge.
- Stvrtinova, V., Jakubovsky, J., Hulin, I., 1995. *The acute phase reactants. Inflammation and Fever*. Academic Electronic Press.
- Takala, A., Jousela, I., Jansson, S.E., Olkkola, K.T., Takkunen, O., Orpana, A., Karonen, S.L., Repo, H., 1999. Markers of systemic inflammation predicting organ failure in community-acquired septic shock. *Clin. Sci. (London)* 97, 529–538.
- Todar, K., 2002. Growth of bacterial populations. In: *Todar's Online Textbook of Bacteriology*. Date Accessed: 10-21-2005. <http://www.textbookofbacteriology.net>.
- Tsukaguchi, K., de, L.B., Boom, W.H., 1999. Differential regulation of IFN-gamma, TNF-alpha, and IL-10 production by CD4(+) alpha-beta TCR+ T cells and vdelta2(+) gammadelta T cells in response to monocytes infected with *Mycobacterium tuberculosis*-H37Ra. *Cell Immunol.* 194, 12–20.
- Wang, H., Bloom, O., Zhang, M., Vishnubhakat, J.M., Ombrellino, M., Che, J., Frazier, A., Yang, H., Ivanova, S., Borovikova, L., Manogue, K.R., Faist, E., Abraham, E., Andersson, J., Andersson, U., Molina, P.E., Abumrad, N.N., Sama, A., Tracey, K.J., 1999. HMG-1 as a late mediator of endotoxin lethality in mice. *Science* 285, 248–251.
- Zouali, M., 2001. Antibodies. In: *Encyclopedia of Life Science*. Nature Publishing Group. Date Accessed: 8-18-2005. www.els.net.